Lars G. Westerberg · **Hans O. Åkerstedt**

2D solutions to the compressible solar wind flow near a reconnection site at the dayside magnetopause

Abstract Magnetic reconnection plays a key role in the transfer of momentum and energy in all applications of space plasma physics. The main physical property of the onset of the process is a breakdown of the frozen-in condition for the solar wind magnetic field. When leaving the Sun, the solar wind has infinite conductivity, i.e. there is no diffusion of field lines within the plasma. Magnetic reconnection is a result of a local diffusion of magnetic field lines, where in the present application, the solar wind magnetic field interact with the terrestrial magnetic field. The objective of the present study is to investigate the behavior of the solar wind flow and magnetic field in the vicinity of a location where magnetic reconnection occurs at the outer boundary of the Earth's magnetic field - the magnetopause. We do not focus on the process itself, but on its implications on the plasma properties during the transition from the magnetosheath region to the magnetosphere. The plasma is considered to have a variable density and is described by the Magneto Hydro Dynamic (MHD) Equations, including non-ideal effects such as viscosity and resistivity. Treating the transition layer at the magnetopause boundary as very thin, the governing equations can be solved approximately by the use of an ordinary perturbation technique, with expansions in orders of large Reynolds and Lundquist numbers. The analysis results in equations describing the plasma properties in the magnetopause transition layer. Analytical solutions have been obtained. These are however only valid in a region close to the reconnection site. In order to extend the region we use FEMLAB to solve the equations.

Keywords Solar Wind Flow · Magnetic Reconnection · Perturbation Theory · FEMLAB - PDE, General Form

Lars G. Westerberg
Division of Fluid Mechanics
Luleå University of Technology
SE-971 87 Luleå, SWEDEN
Tel.: +46-920-491268
Fax: +46-920-491047
E-mail: lgwe@ltu.se

Hans O. Åkerstedt
Division of Fluid Mechanics
Luleå University of Technology
SE-971 87 Luleå, SWEDEN
Tel.: +46-920-491280
Fax: +46-920-491047
E-mail: hake@ltu.se

1 Introduction

Magnetic reconnection is the main mechanism for the transfer of momentum and energy in all plasma physical applications. It was until the beginning of the 1960's when the theory of magnetic reconnection was presented, a riddle how magnetic energy was transformed to kinetic energy. Since the onset of the theory of magnetic reconnection a lot of questions has been answered. This topic has though gone through a journey where it at some times reached almost mythical proportions, to the position it has today, where much of the research has its focus on the main onset mechanisms. Whether reconnection do occur or not, is not anymore a victim of the debate. Rather the implications of the process on the plasma properties.

Throughout the years it has been made an enormous amount of work treating this topic. In recent years, i.e. during the last decade much of the work has its focus on satellite data analysis, numerical analysis and MHD simulations. This due to the fast increase in computer capacity. In these works a usual simplifying approximation is to treat the plasma as incompressible.

The present work is an extension of the two-dimensional analysis made by [7], which in turn is a development of the ideas presented by [5], treating an incompressible study of the interaction between the solar wind and the terrestrial magnetopause. There, magnetic reconnection is assumed to occur at an arbitrary point in a region stretching from the sub-solar point to the north. The main issue of the present study is not the reconnection process itself, but rather the implications of it; how the plasma properties such as the magnetic field and plasma velocity develops during the transition from the magnetosheath to the magnetosphere.

The plasma motion is described by the MHD equation of motion, together with the continuity equation, while the induction equation and the solenoidal properties of the magnetic field govern the magnetic field. We use a curvilinear coordinate system with the common used labels for the coordinate axis, i.e. z being the tangential component along the magnetopause surface and x the normal component. See Fig. 1.

The current transition layer is treated as very thin, allowing us to solve the governing equations approximately by the use of an ordinary perturbation expansion

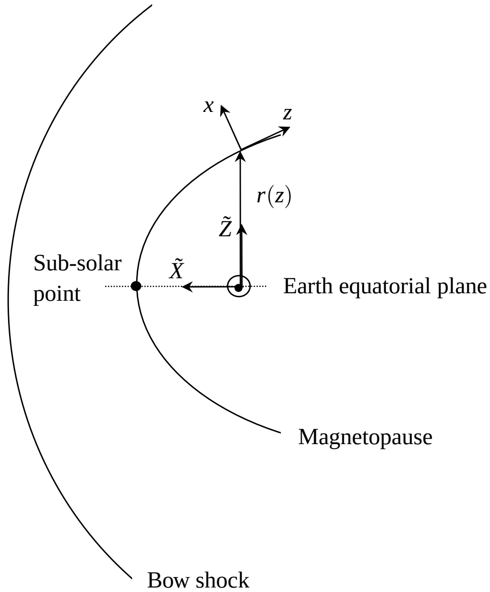

Fig. 1 The curvilinear coordinate system. The conventional coordinate system in space physics is used, i.e. x pointing normal to the magnetopause surface and the z-component lying in the tangential direction of the magnetopause. This means that at the sub-solar point x points towards the sun and z towards the geographical north. The coordinate-system with origin at the center of the Earth is used for the development of the parabolical unit vectors ($\hat{u}$, $\hat{v}$ and $\hat{\phi}$) in terms of the curvilinear coordinates x, y, and z. Here $r(z) = p \cdot \rho^{-\gamma} =$ constant (p is the pressure, ρ the density, and γ the specific heat ratio), for two dimensions [4], and for three dimensional axisymmetry $r(z)$ is the distance in the figure. From [5] and [6].

in terms of large Reynolds (R) and Lundqvist (L_u) numbers, where

$$R = \frac{v_A \cdot R_E}{\nu} \tag{1}$$

and

$$L_u = \frac{v_A \cdot R_E}{\eta}. \tag{2}$$

R_E is the Earth radius and v_A the Alfvén velocity of the tangential magnetic field component at a given reference point. ν is the viscosity of the plasma, and η the magnetic diffusivity. Since the plasma is mainly collisionless, viscosity and resistivity are not appropriate in a classical sense. We can though treat them as anomalous transport coefficients. The kinematic viscosity and diffusivity are estimated to be of the same order ($= 10^{13}\mathrm{cm}^2/\mathrm{s}$) [1] [3].

2 Governing equations and method of solution

The equations governing the plasma motion and magnetic field are the steady MHD equation of motion, the induction equation, the solenoidal property of the magnetic field, and the continuity equation

$$\rho(\mathbf{u}\cdot\nabla)\mathbf{u} = \mu\nabla^2\mathbf{u} - \nabla \mathrm{P} + \frac{1}{\mu_0}(\mathbf{B}\cdot\nabla)\mathbf{B} \tag{3a}$$

$$\frac{\partial \mathbf{B}}{\partial t} = \nabla\times(\mathbf{u}\times\mathbf{B}) + \frac{1}{\mu_0\sigma}\nabla^2\mathbf{B} \tag{3b}$$

$$\nabla\cdot\mathbf{B} = 0 \tag{3c}$$

$$\nabla\cdot(\rho\mathbf{u}) = 0 \tag{3d}$$

where P is the total pressure

$$\mathrm{P} = \mathrm{p} + \frac{\mathrm{B}^2}{2\mu_0} \tag{4}$$

and $\rho = \rho(x,z)$. Considering a two dimensional steady flow, we let

$$\mathbf{u} = u_x\hat{\mathbf{x}} + u_z\hat{\mathbf{z}} \tag{5a}$$

$$\mathbf{B} = B_x\hat{\mathbf{x}} + B_z\hat{\mathbf{z}}. \tag{5b}$$

The transition layer separating the magnetosheath plasma from the magnetosphere plasma is assumed thin, so δ^* is introduced as a characteristic thickness. The length scale in the main flow direction (z) is taken as L. One choice of L being the Earth radius R_E. A small parameter δ

$$\delta = \frac{\delta^*}{R_E} \ll 1 \tag{6}$$

is chosen.

An order of magnitude estimate shows that as in ordinary boundary layer theory the thickness scales as

$$\delta = O(R^{-\frac{1}{2}}). \tag{7}$$

2.1 The DeHoffmann-Teller frame of reference and the fast variable ξ

The absolute velocity, now denoted u_z^*, is divided into a DeHoffmann-Teller velocity U_{HT} and u_z, the velocity with respect to the DeHoffmann-Teller frame of reference [2],

$$u_z^* = u_z + U_{HT}. \tag{8}$$

In the DeHoffmann-Teller frame the y-component of the electric field is zero, implying that particles do not change their kinetic energy when passing through the current sheet from one side to the other. In this frame of reference the plasma properties are the same in the magnetosheath and the boundary layer, except for the magnetic field and the direction of the plasma flow.

Recalling that

$$\frac{\partial}{\partial x} = O(R^{\frac{1}{2}}) \tag{9}$$

we introduce the new fast variable ξ

$$\xi = R^{\frac{1}{2}} \cdot x. \tag{10}$$

This gives

$$\frac{\partial}{\partial x} = R^{\frac{1}{2}} \frac{\partial}{\partial \xi} \tag{11a}$$

$$\frac{\partial^2}{\partial x^2} = R \frac{\partial^2}{\partial \xi^2}. \tag{11b}$$

U_{HT} is chosen such that

$$E_y + U_{HT} \cdot B_\xi = 0 \tag{12}$$

where E_y for two dimensions can be verified to be constant.

2.2 The perturbation expansion

In order to have a possibility to let the normal components of the magnetic field and velocity to be small, they are assumed to be of order $O(R^{-\frac{1}{4}})$. This means that in the limit of large R, they are always larger than the ordering of the current sheet thickness of order $O(R^{-\frac{1}{2}})$. The following ansatz for the perturbation expansion leads to no inconsistencies, and results in a sequence of equations to different separate order.

$$u_\xi = R^{-\frac{1}{4}} \cdot u_\xi^{(0)} + R^{-\frac{1}{2}} \cdot u_\xi^{(1)} + \ldots \tag{13a}$$

$$u_z = U_{HT} + u_z^{(0)} + R^{-\frac{1}{4}} \cdot u_z^{(1)} + \ldots \tag{13b}$$

$$B_\xi = R^{-\frac{1}{4}} \cdot B_\xi^{(0)} + R^{-\frac{1}{2}} \cdot B_\xi^{(1)} + \ldots \tag{13c}$$

$$B_z = B_z^{(0)} + R^{-\frac{1}{4}} \cdot B_z^{(1)} + \ldots \tag{13d}$$

$$\rho(\xi,z) = \rho^{(0)}(z) + R^{-\frac{1}{4}} \cdot \rho^{(1)}(\xi,z) + \ldots \tag{13e}$$

$$E_y = R^{-\frac{1}{4}} \cdot E_y^{(0)} + R^{-\frac{1}{2}} \cdot E_y^{(1)} + \ldots \tag{13f}$$

Since we consider a resolution of a rotational discontinuity the density is to the lowest order constant across the transition layer. The Lundqvist number is assumed to be of the same order as the Reynolds number.

Applying (13) to (3) results together with the relation between the Alfvén velocity and the speed of sound

$$\frac{{B_\xi^{(0)}}^2}{\mu_0 \rho^{(0)}} << \frac{\gamma \cdot p^{(0)}}{\rho^{(0)}} \tag{14}$$

in the equation describing the plasma behavior in the magnetopause current sheet

$$\left(1 + \rho^{(0)} \frac{R}{L_u}\right) \frac{\partial^2 u_z^{(0)}}{\partial \xi^2} + \frac{\partial u_z^{(0)}}{\partial \xi} \left[2\xi \frac{1}{r(z)} \frac{\mathrm{d}}{\mathrm{dz}} (r(z) \right.$$

$$\left. \rho^{(0)} U_{HT}) - \frac{1}{r(z)} \frac{\mathrm{d}(r(z)\rho^{(0)})}{\mathrm{dz}} \int_{-\infty}^{\xi} u_z^{(0)} \, \mathrm{d}\xi \right] -$$

$$2\rho^{(0)} U_{HT} \frac{\partial u_z^{(0)}}{\partial z} - \rho^{(0)} U_{HT} \frac{\mathrm{d}U_{HT}}{\mathrm{dz}} - \frac{\partial P}{\partial z} +$$

$$u_z^{(0)2} \frac{\mathrm{d}\rho^{(0)}}{\mathrm{dz}} + \frac{1}{2} u_z^{(0)} U_{HT} \frac{\mathrm{d}\rho^{(0)}}{\mathrm{dz}} = 0. \tag{15}$$

The DeHoffmann-Teller velocity is different north and south of the reconnection point, resulting in one equation for each case.

3 Solutions

In order to solve (15) we use FEMLAB[1] and its PDE-General form application, which in addition to the coefficient form, is better suited for nonlinear problems. We begin though with the analysis resulting in the expressions for the plasma properties (i.e. velocity and density) at the outer magnetopause boundary.

3.1 Plasma properties at the outer magnetopause boundary

The expressions for the density and velocity variation at the outer magnetopause boundary are based on simulation studies of a gas-dynamic flow around an obstacle. Since not including a magnetic field, these results are not ideal for the present application. Still, they can be used as a working hypothesis.

3.1.1 Density variation

From [7] the variation of the density along the magnetopause is given by

$$\rho(u) = 1.509 \cdot \exp\left(1 - \frac{u}{R_{mp}}\right) \tag{16}$$

where u is a parabolical coordinate, and R_{mp} the stand-off distance to the magnetopause. By applying a Taylor expansion at the reconnection site ($u = u_0$) and using the relation between the curvilinear coordinate Z and the parabolical coordinate u

$$u - u_0 = \frac{2}{R_{mp}} \sqrt{\frac{u_0}{1+u_0}} \cdot Z \tag{17}$$

we obtain an expression for the density on the form

$$\rho(Z) = A + B \cdot Z + C \cdot Z^2 + D \cdot Z^3. \tag{18}$$

[1] FEMLAB 3.1i, is used in this analysis

In order to extend the solution domain we consider a higher order expansion up to $O(Z^3)$, in comparison to the theoretical analysis which only treat up to order $O(Z)$. A-D are constants whose numerical value is determined by u_0 and R_{mp}. We consider the reconnection site to be located at two R_E from the sub-solar point. This corresponds to $u_0 = 0.13$, given by the relation

$$Z(u) = \frac{R_{mp}}{2} \int_{u_0}^{u} \sqrt{\frac{1+u}{u}}\, du \tag{19}$$

from [5]. $R_{mp} = 10$ is a standard value, and used in every case in this study.

3.1.2 The DeHoffmann-Teller velocity

In accordance to the 2D and 3D study [6] and [7], the plasma velocity and magnetic field along the magnetopause are given by

$$U_z^* = 2.89 \cdot M_A R_{mp} \cdot \ln\left(1 + \sqrt{\frac{2u}{R_{mp}}}\right) \tag{20a}$$

$$B_z^* = -R_{mp}\sqrt{\frac{u}{u+1}}. \tag{20b}$$

where M_A is the local Alfvénic Mach number at the reconnection site

$$M_A = \frac{V_\infty \frac{\rho_\infty}{\rho} \sqrt{\mu_0 \rho(0)}}{B_x^{imf}}. \tag{21}$$

Here V_∞ and ρ_∞ are the velocity and density in the unshocked solar wind. North and south of a reconnection point the relation between the velocities and the magnetic field are

$$U_z^* = B_z^* + U_{HT}^{\mathrm{N}} \tag{22a}$$

$$U_z^* = U_{HT}^{\mathrm{S}} - B_z^*. \tag{22b}$$

Index N and S corresponds to north and south respectively. By expanding the terms in a Taylor series as in the case for the density, we obtain expressions for the DeHoffmann-Teller velocities of the same character as (18).

3.1.3 The pressure gradient and magnetopause radius of curvature

By studying the z-component of the inviscid limit (i. e. $R \to \infty, \frac{\partial}{\partial x} \to \infty$) of the MHD equation of motion we have

$$-\frac{\partial P}{\partial z} = \rho \cdot U_z^* \frac{dU_z^*}{dz} - B_z^* \frac{dB_z^*}{dz} \tag{23}$$

where ρ, U_z^* and B_z^* are according to (18) and (20). The magnetopause radius of curvature is according to [5]

$$r(z) = R_{mp}\sqrt{u}. \tag{24}$$

As for the previous quantities we use a Taylor expansion at the reconnection site together with (17).

3.2 Solving methodology

In the FEMLAB - PDE General Form tool, the basic stationary equation is of the form

$$\nabla \cdot \Gamma = F \tag{25}$$

where Γ and F are vectors such that

$$\Gamma = \begin{bmatrix} \Gamma_1 \\ \vdots \\ \Gamma_n \end{bmatrix} \tag{26a}$$

$$F = \begin{bmatrix} F_1 \\ \vdots \\ F_n \end{bmatrix} \tag{26b}$$

for an equation system with n dependent variables. The procedure for solving (15) is straightforward. In order to include the integral term

$$\int_{-\infty}^{\xi} u_z^{(0)}\, \mathrm{d}\xi \tag{27}$$

we introduce a new variable $v = v(\xi, Z)$ such that

$$\frac{\partial v}{\partial \xi} = u_z^{(0)}. \tag{28}$$

This results in

$$\int_{-\infty}^{\xi} u_z^{(0)}\, \mathrm{d}\xi = v(\xi, Z). \tag{29}$$

In FEMLAB $u_z^{(0)}$ and v are represented by u_1 and u_2 respectively. Furthermore, ξ and z are represented by x and y in the actual geometry. The derivatives are denoted with u_x and u_y. (15) is then expressed in Γ and F such that

$$\begin{aligned} \Gamma_1 &= (1+\rho^{(0)}) \cdot u_{1x}\, \hat{\mathbf{x}} \\ \Gamma_2 &= 0 \end{aligned} \tag{30a}$$

$$\begin{aligned} F_1 = &-\Big[2x \cdot \frac{1}{r(z)}\frac{d}{dz}(r(z)\rho^{(0)}U_{HT}) - \\ &\frac{1}{r(z)}\frac{d}{dz}(r(z)\rho^{(0)}) \cdot u_2\Big] \cdot u_{1x} + 2\rho^{(0)}U_{HT} \cdot u_{1y} + \\ &\rho^{(0)}U_{HT}\frac{dU_{HT}}{dz} + \frac{dP}{dz} - \frac{d\rho^{(0)}}{dz} \cdot u_1^2 - \\ &\frac{1}{2}u_1 U_{HT}\frac{d\rho^{(0)}}{dz} \end{aligned} \tag{30b}$$

$$F_2 = u_1 - u_{2x}. \tag{30c}$$

We consider a geometry in form of a rectangle where $-5 \leq x \leq 5$, $0 \leq y_N \leq 1.5$ and $-1.5 \leq y_S \leq 0$. N and S represents as earlier north and south of the reconnection site respectively. x and y corresponds to ξ and Z in the analysis. The actual boundary conditions are homogeneous Neumann conditions for u_1 at all sides except for $y = 0$, where we have a start condition of the form

$$u_1 = C_1 \cdot \mathrm{erf}(\alpha \cdot x) \tag{31}$$

where C_1 is a constant whose numerical value is obtained by asymptotic matching of the magnetic field [7]. In order to have a transition of the magnetic field in accordance with the structure indicated by the theoretical analysis, we treat the case where $\alpha = 5$. $u_2 = 0$ at $x = -5$, while it satisfies homogeneous Neumann conditions at the other boundaries.

4 Results

In this section we present the solutions to (15) obtained with FEMLAB. Following parameter values are considered:

$$V_\infty = 300 \text{ km/s} \tag{32a}$$

$$\rho_\infty = 5 \text{ cm}^{-3} \tag{32b}$$

$$B_x^{imf} = 18 \text{ nT} \tag{32c}$$

$$R_{mp} = 10. \tag{32d}$$

In order to compare with the analytical solutions [7], we consider the cross-sectional plots at different locations. Since we with FEMLAB can include higher order terms in the expansions of each quantity, the region where the solutions are valid is extended. In this study $z_{max/min.} = \pm 1.5$ (positive sign corresponding to north of the reconnection site), which should be compared with the analytical solutions where z stretches to roughly ± 0.5. The development of the magnetic field north of the reconnection site is viewed in Fig. 2.

The structural behavior is in analogy with the results in [7]. Still, the development differs for the two approaches due to a smaller region where the analytical solutions are valid. For small z the analytical solution satisfies the numerical solution. See Fig. 3 for corresponding development south of the reconnection point.

For this case the magnetic field experiences the same development structure up to $z \approx 0.5$ as north of the reconnection point. Thereafter the deviation is more significant. North of the reconnection site the plasma velocity and magnetic field increases faster due to a positive gradient. This property should reasonably play a crucial role for the evolution of respective quantity. For the corresponding behavior of the total velocity (U^*) north of the reconnection site, see Fig. 4.

The evolution of the total velocity for positive z follows the same pattern the analytical results do for small z. However with a slight modification in the structure of the solution. The deviation from the start condition at the reconnection site, is more distinct for growing z. The distribution of the total velocity south of the reconnection site is showed in Fig. 5.

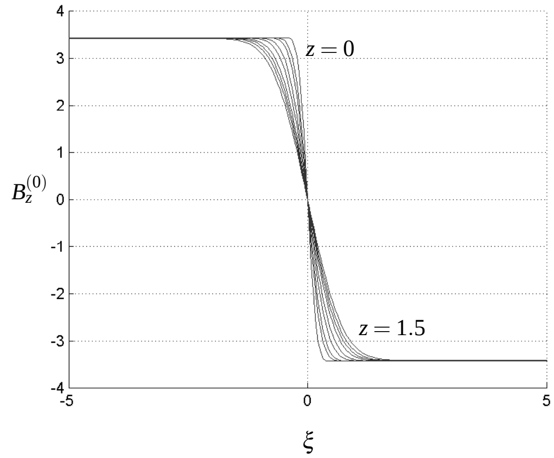

Fig. 2 Evolution of the magnetic field ($B_z^{(0)}$) north (positive z) of the reconnection site when the plasma travels through the magnetopause boundary. Positive ξ corresponds to the outer region, i.e. the magnetosheath. Negative ξ correspondingly represents the inner region, i.e. the magnetosphere. Respective curve represent the development at different locations ($z = 0$, $z = 0.1$, $z = 0.2$, $z = 0.3$, $z = 0.5$, $z = 0.8$, $z = 1$ and $z = 1.5$) from the reconnection site ($z = 0$). The analytical solutions [7] are valid to $z \approx 0.5$.

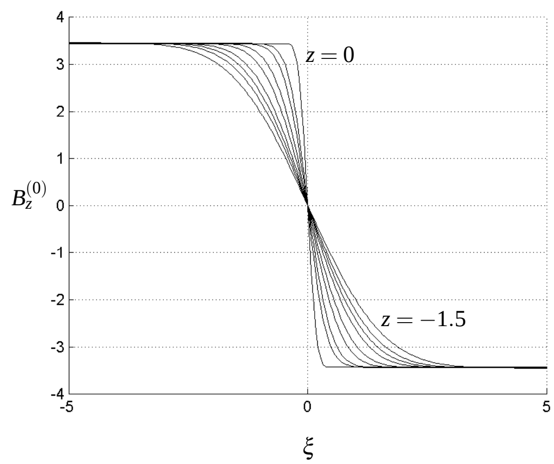

Fig. 3 Evolution of the magnetic field ($B_z^{(0)}$) south (negative z) of the reconnection site when the plasma travels through the magnetopause boundary. As for the case north of the reconnection point, positive ξ corresponds to the outer region and negative ξ the inner region. The development of the magnetic field is viewed at following locations: $z = 0$, $z = -0.1$, $z = -0.2$, $z = -0.3$, $z = -0.5$, $z = -0.8$, $z = -1$ and $z = -1.5$.

As for the previous case north of the reconnection site, the theoretical result is in coherence with the present one. The total velocity develops continuously for $z \geq 0.525$. Comparing the development of respective total velocity, we notice a discontinuous behavior at the reconnection site ($z = 0$). This due to the DeHoffmann-Teller velocity (U_{HT}) which is not well defined at this point.

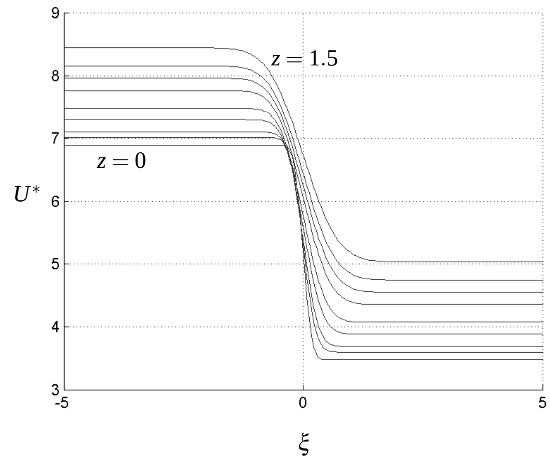

Fig. 4 Development of the total velocity ($U^* = u_z^{(0)} + U_{HT_N}$) north of the reconnection point. As earlier the respective curves represents the development at different locations ($z = 0$, $z = 0.1$, $z = 0.2$, $z = 0.3$, $z = 0.5$, $z = 0.8$, $z = 1$ and $z = 1.5$) from the reconnection site ($z = 0$).

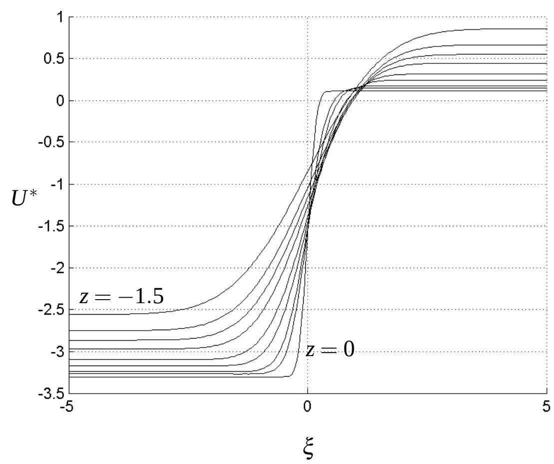

Fig. 5 Development of the total velocity ($U^* = u_z^{(0)} + U_{HT_S}$) south of the reconnection point. Comparing the development of respective total velocity, we notice a discontinuous behavior at the reconnection site ($z = 0$). This due to the DeHoffmann-Teller velocity (U_{HT}) which is not well defined at this point. South of the reconnection point z is negative. Following locations are considered: $z = 0$, $z = -0.1$, $z = -0.2$, $z = -0.3$, $z = -0.5$, $z = -0.8$, $z = -1$ and $z = -1.5$.

5 Summary

This work treat the interaction between the solar wind and the outermost layer of the terrestrial magnetic field - the magnetopause. Magnetic reconnection is a process of certain interest. It is supposed to occur in a region stretching from the sub-solar point to the north. The focus does not lie in the process itself, but on its implications on the plasma behavior in the vicinity of a location where reconnection is initiated. We consider a plasma with variable density. The transition layer separating plasma from the magnetosheath- and the magnetosphere region is viewed as a large amplitude Alfvén wave. Thereby the only effect is a rotation of the magnetic field during the transition from the magnetosheath to the magnetosphere. Thus the density can be treated to be the same at the immediate sides of the magnetopause boundary. Viscosity and resistivity are included as non-ideal effects. In order to solve the the magnetohydrodynamic equations which govern the plasma flow and magnetic field, we use an ordinary perturbation technique with expansion in large Reynolds and Lundqvist numbers. This results in equations describing the plasma properties north and south of a location where reconnection occurs. In order to solve these equations and to extend the region where the solution is valid in addition to previous theoretical work, we use FEMLAB. The results are compared with the analytical solutions. It is shown that the structural behavior is the same as for the analytical solutions for small distances away from the reconnection site. However, the magnetic field and total velocity develops differently for large distances away from the reconnection site. A comparison with the analytical solutions for the case of an incompressible solar wind plasma, also shows a deviation in the behavior when moving further away from the reconnection site. Even in this case the difference is clearly visible for larger distances.

Acknowledgements This work is financed through the Swedish National Graduate School of Space Technology.

References

1. Axford, W. I. Viscous interaction between the solar wind and the Earth's magnetosphere. *Planet. Space Sci.* **12**, 45-53 (1964).
2. DeHoffmann, F., Teller, E. Magnetohydrodynamic shocks. *Phys. Rev. Lett.*, **80**, 692 (1950).
3. Haerendel, G., Paschmann, N., Sckoke, N., Rosenbauer H. The front side boundary layer of the magnetosphere and the problem of reconnection. *J. Geophys. Res.*, **83**, 3195 (1978).
4. Schlichting, H. Boundary Layer Theory *McGraw-Hill Series in Mechanical Engineering, New York, USA* (1979)
5. Westerberg, L. G. and Åkerstedt, H. O. A two dimensional analysis of the flow past an open terrestrial magnetopause *J. Plasma Phys.*, **71**, 5 (2005) .
6. Westerberg, L. G. and Åkerstedt, H. O. A three dimensional analysis of the flow past an open terrestrial magnetopause *J. Plasma Phys.* (accepted for publication) (2005).
7. Westerberg, L. G., Solar wind interaction with the terrestrial magnetopause, 87-109. *Luleå University of Technology, Licentiate Thesis. Luleå, Sweden* (2005).